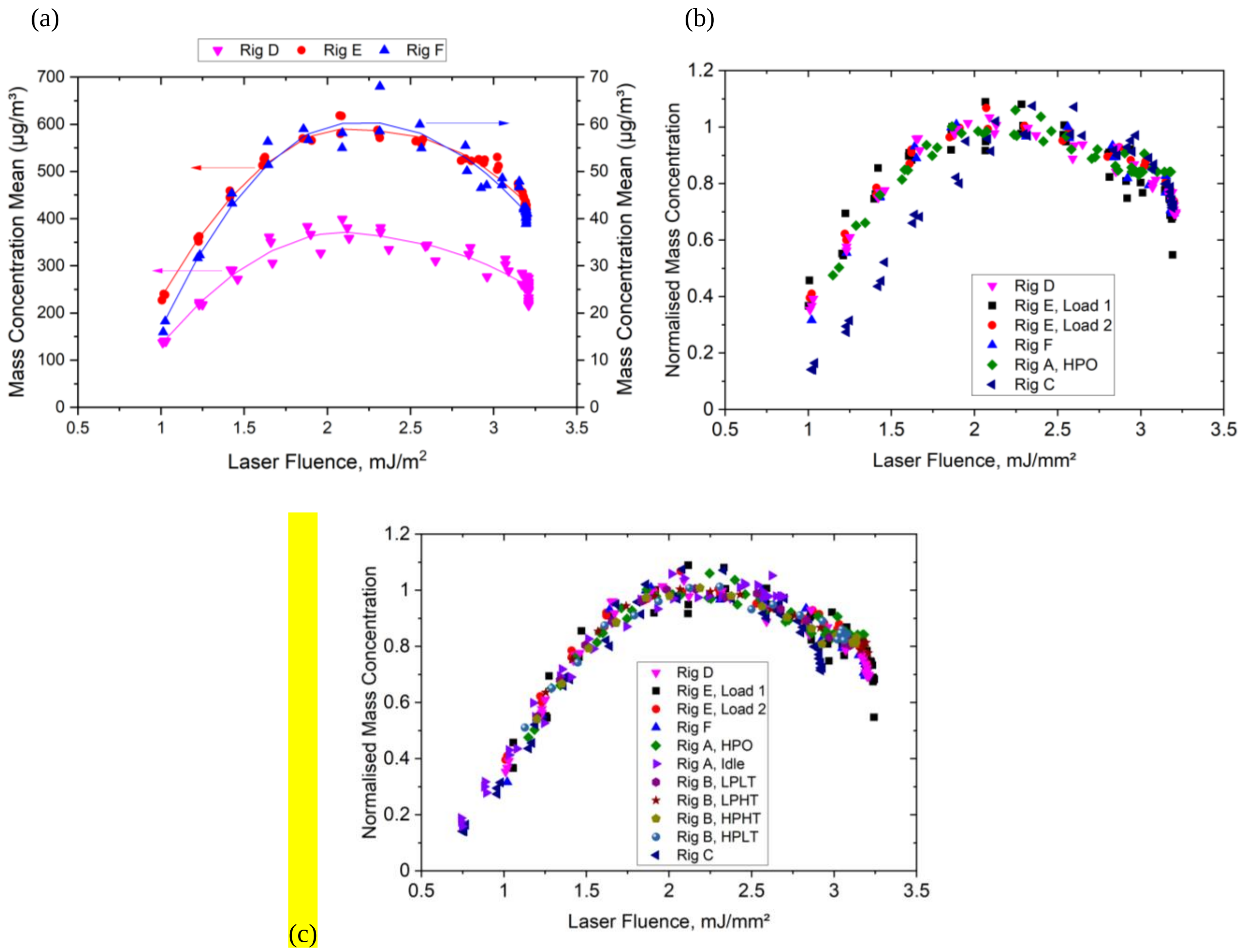

Fig. 11. (a) Laser fluence dependence of mass concentration measurements from LII 300 using multiple nvPM sources from diesel (Rigs D and E Load 2) and gasoline (Rig F) fuelled engine exhausts at typical operation conditions. Superimposed are the best-fit curves from the Loess method. (Arrows point at the corresponding Y-axis.) (b) Normalised mass concentration vs laser fluences from Rigs A and C to F. Measurements were carried out by the same instrument LII 1 for the kerosene cases (Rigs A, C) as for the diesel and gasoline cases (Rigs D to F). Rig E, Load 1: speed 1200 rpm, load 165 Nm and Load 2: speed 2200 rpm, load 300 Nm. (c) Combined data from Rig A (idle) and Rig B (at four conditions shown in Fig. 9b) to (b), the laser fluence axis of Rig C and Rig E, Load 1 was left-shifted by 0.27 and - 0.05 mJ/mm^2, respectively.

In general, similar behaviour is observed in the normalised data from all the rigs and fuels in the plateau ranges. Fig. 11(b) illustrates that the optimum fluence from Rig A overlaps well with that from other rigs, except for Rig C. The results from Rig C require a shift on the fluence axis (of around 0.3 mJ/m^2) in order to align with those from Rig A (HPO condition), as shown in Fig. 9c where the fluence data from six rigs and a total of 11 conditions converge after the fluence shifts were applied. This shift was due to the combustion formed soot particles emitted from Rig C which had different physical and chemical characteristics compared to the soot formed from Rig A. Further analysis would require much greater understanding of the soot morphology, structure, and composition characteristics from the various operation conditions, which is beyond the scope of this paper.